PST-06-59
PPT-06-42

Operation Mode of Oversized Backward Wave Oscillator Driven by Weakly Relativistic Electron Beam

K. Ogura, Y. Miyazawa, Y. Kiuchi, S. Aoyama, H. Tanaka and A. Sugawara
Graduate School of Science and Technology, Niigata University
8050 Igarashi Ninocho, Niigata 950-2181, Japan

Abstract

We study the operation mode of oversized BWO driven by weakly relativistic electron beams less than 100 kV. In experiments, the performance of oversized BWOs is improved by improving the SWS and the beam shape. The output power increases up to about 500 kW in K-band and about 200 kW in Q-band, which corresponds to the quality factor Pf^2 of about 3.5×10^5 kW·GHz^2. High-power operations in the nonaxisymmetric mode are observed. To analyze the oversized BWO, a new version of linear theory is used, in which three-dimensional beam perturbation are self-consistently considered. For the oversized SWS, the electromagnetic waves are surface waves localized near the SWS wall. Two kinds of beam interaction, slow cyclotron and Cherenkov interactions, exist in the oversized BWO as in the non-oversized BWO. The nonaxisymmetric mode can be excited by the completely axisymmetric beam in the completely axisymmetric system. The growth rate of nonaxisymmetric mode is in the same order as the axisymmetric mode. If the beam is apart from SWS, the growth rates decrease exponentially. The beam radius should be controlled carefully to drive oversized BWOs.

Keywords: oversized backward wave oscillator, weakly relativistic beam, axisymmetric mode, nonaxisymmetric mode

I. Introduction

Slow-wave high-power microwave devices such as backward wave oscillator (BWO) can be driven by an axially injected electron beam without initial perpendicular velocity and has been studied extensively as a candidate for high power microwave sources [1]. In the slow-wave devices, a slow-wave structure (SWS) is used to reduce the phase velocity of electromagnetic wave to the beam velocity. In order to increase the power handling capability and/or the operating frequency, oversized SWSs have been used successfully [2-9]. The term "oversized" means that the diameter D of SWS is larger than free-space wavelength λ of output electromagnetic wave by several times or more. In this work, operation modes of oversized BWO are studied experimentally and theoretically. Our BWOs are driven by a weakly relativistic electron beam less than 100 kV and are operating in relatively high frequency region, above 10 GHz. Note that high-power operations beyond 10 GHz are difficult for the conventional non-oversized slow-wave devices.

II. Oversized SWS

Figure 1 shows a schematic diagram of large diameter SWS module used in our experiments. The wall radius of the structure $R_w(z)$ varies sinusoidally along the axial direction z as $R_0+h\cos(k_0z)$. Here, $k_0=2\pi/z_0$ is a corrugation wave number. Each module consists of ten periods. Parameters of SWS are listed in Table 1. The values of λ in the table are estimated with the operation frequency at the axial wave number $k_z=k_0$. Since the inner wall of the SWS is spatially periodic with k_0, the fields in SWS are expressed by a sum of Floquet's harmonic series. The axial electric field becomes

$$E_z = \sum_{p=-\infty}^{\infty} A_p J_m\left(x_p r\right)\exp\left(ik_p z + im\theta - i\omega t\right). \quad (1)$$

Here, $x_p^2=\omega^2/c^2-k_p^2$, $k_p=k_z+pk_0$ and p is the spatial harmonic number. J_m is the normal function of cylindrical system, i.e., the mth order Bessel function of the first kind. Using the boundary conditions at the wall, the normal electromagnetic modes of the system can be derived [10-13].

The dispersion characteristics of the structure are controlled by changing average diameter D_0, corrugation amplitude h and pitch length z_0. The upper cutoff of the lowest mode is mainly determined by h and the lower cutoff

Table 1 Parameters of the periodic SWS

	D_0[mm]	h_0[mm]	z_0[mm]	λ[mm]	D_0/λ
K-Band	31.4	1.7	3.4	12.4	2.4
Q-Band	30.0	1.0	2.0	7.46	4.0

is determined by D_0. In frequency domain, the modes are overlap and are not separated by stop-bands. This is in contrast to the non-oversized cases, for which the modes are well separated and have well defined band-pass characteristics.

The dispersion curves of lowest modes, HE_{11}, TM_{01} and HE_{21} mode, are shown in Fig.2. And, the field profile of HE_{11} near the operation point is shown in Fig.3. For the oversized SWS, the operation point is much below the light line and the field properties near the operation point are mainly determined by h and z_0. All the spatial harmonics are expressed by the modified Bessel function with $x_p^2<<0$ and are evanescent waves in the radial direction. The spatial harmonics with p=0 and -1 play the main role in the beam interaction with electromagnetic waves and are also evanescent in the radial direction. The field decreases sharply from the SWS wall and is glued to the wall. The electromagnetic modes are surface waves as shown in Fig.3.

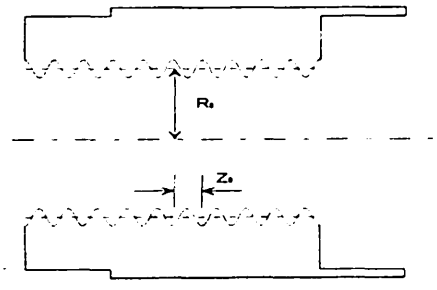

Fig.1 Schematic diagram of SWS modular used in the oversized BWO experiments. The wall radius $R_w(z)$ varies along the axial direction z as $R_0+h\cos(k_0z)$, where $k_0=2\pi/z_0$.

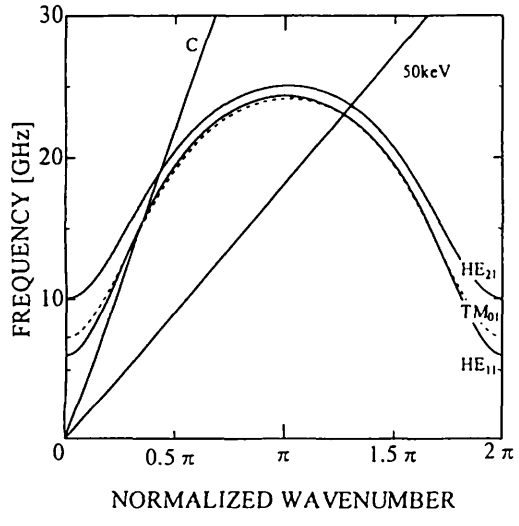

Fig.2 Dispersion curves of HE_{11}, TM_{01}, and HE_{21}. As a reference, 50 keV beam line and light line are plotted.

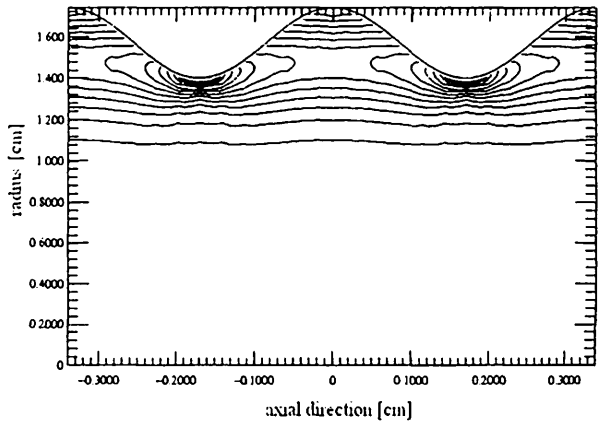

Fig.3 Distribution of |E| of HE_{11} mode in K-band SWS at the π point

For an efficient beam interaction with the surface wave, the beam should propagate near the wall and the interacting point between the beam and electromagnetic wave is shifted to the π point. The π point means the upper edge of the lowest mode with $k_zz_0=\pi$ in Fig.2. In our oversized SWS, the beam less than 100 kV will couple to the backward electromagnetic modes near the π point. The operation frequency is in the ranges of 20 GHz (K-band) and 40GHz (Q-band). The SWS is oversized with $D_0/\lambda\approx2.4$ (K-band) and $D_0/\lambda\approx4$ (Q-band), as listed Table 1.

III. Experiment

In this section, the results of oversized BWO experiment are presented. The microwave output is picked up by a rectangular horn antenna located away from the output window. Received signals are split into two branches for the frequency measurement. One forms a prompt signal. The other forms a delayed signal, by passing through a delay line. The microwave frequency is able to estimate from the delay time between prompt and delayed signals.

Figure 4 shows an example of detected signals of K-band BWO. The beam voltage and current at the time of microwave peak are about 90 kV and 300 A, respectively. From the delay time between prompt and delayed microwave signals, the radiation frequency is estimated to be about 23 GHz.

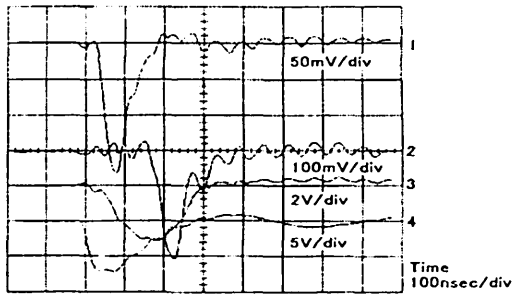

Fig.4 Time history signals: 1 prompt signal, 2 delayed signal, 3 beam current and 4 beam voltage.

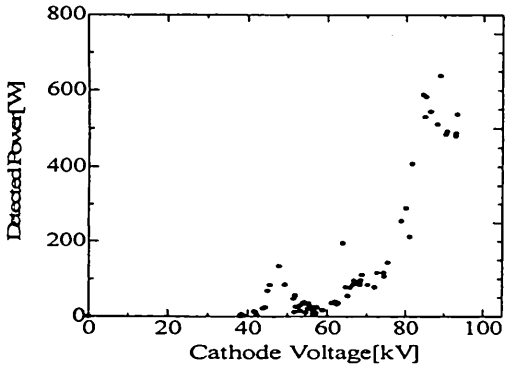

Fig.5 Output power versus the cathode voltage for K-band SWS. The magnetic field is 0.8 T.

Figure 5 shows the dependence of the detected microwave power on the beam voltage for the K-band BWO. There exists the starting energy for the oversized BWO, above which the meaningful radiation is observed [7-9]. For the K-band BWO with $L=20z_0$, the starting energy is around 40 keV. Output powers increase by increasing the beam voltage, i.e. by shifting the beam interacting point to the point of $k_z z_0=\pi$. The estimated radiation power level is about 40kW in the range 40-50kV. Above 70-80 kV, the radiation power increases up to 100 kW level. The same features are observed in the oversized Q-band BWO experiment. The estimated power level of the Q-band BWO is 20 kW in the range 40-50kV. Above 70-80 kV, the power increases to about 50-60 kW. The quality factor Pf^2 of oversized BWOs is about 2×10^4 [kW·GHz^2] in the range of 40-50 kV. This factor increases to about 6×10^4 [kW·GHz^2], by increasing the beam voltage above 70-80 kV.

The power is not improved above 6×10^4 [kW·GHz^2], only by increasing beam voltage. To realize the stable operation higher than 6×10^4 [kW·GHz^2], we need to improve SWS and beam shape. With the improved annular beam and SWS, the powers increase to about 500 kW (K-band BWO) and 200 kW (Q-Band BWO), with 90-100 kV beam voltage. The quality factor Pf^2 is about 3.5×10^5 [kW·GHz^2].

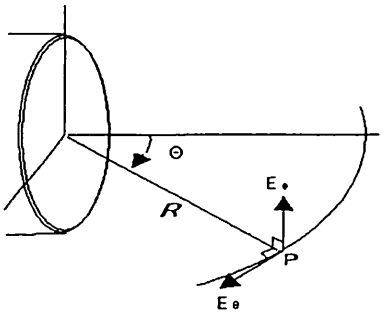

Fig.6 Radiation pattern measurement. Antenna is located at point P in a equatorial plain.

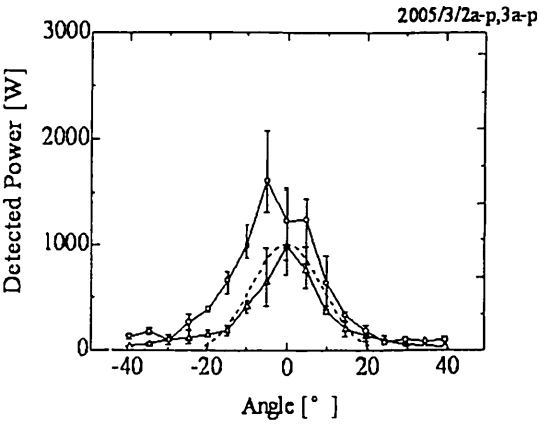

Fig.7 Example of radiation pattern for a high-power oversized BWO; with E_θ (○) and E_φ (△) polarization. The beam voltage and current are respectively about 90 kV and 300 A. The magnetic field is 0.8 T.

The measured frequencies of 20-24 GHz (K-band BWO) and 35-43 GHz (Q-band BWO) are in agreement with the frequencies predicted from the fundamental TM_{01}, HE_{11} or HE_{21} mode in Fig.3. From the frequency measurement, we cannot uniquely determine the operation mode. The radiation patterns are measured by scanning the receiving horn antenna in an equatorial plane around a pivot at the center of output window as shown Fig.6. The electric fields are measured with θ and φ polarization, which are E_θ and E_φ in Fig.6, respectively. Figure 7 shows an example of radiation pattern for a high power operation of the K-band BWO. The radiation pattern is quite different from TM_{01}. The patterns with θ and φ polarizations clearly show the characteristic feature of TE_{11}. A peak at the center θ=0 can be explained only by TE_{11} mode. There is no peak at the center for TM_{mn} and other TE_{mn} radiations. The power levels at θ=0 of E_θ and E_φ are nearly the same. This may be explained by the rotating TE_{11} component. The radiation mode observed is nonaxisymmetric hybrid mode with the azimuthal index m=1, which is a sum of TM_{11} and TE_{11} components. The main peak at θ=0 is due to the TE_{11} component. The TM component contributes the broadening or side peaks of the pattern.

IV. Theoretical Analysis of Operation Modes

In this section, operation modes of oversized BWO are numerically studied by using a new version of linear theory developed in Refs. [10-12], which is considering the three-dimensional beam perturbations and boundary conditions self-consistently. The radial displacement is taken into account properly. Nonaxisymmetric as well as axisymmetric beam instabilities in oversized SWS are investigated. We consider large diameter SWS with the parameter corresponds to our oversized BWO. A magnetic field B_0 is applied uniformly in the axial direction. An electron beam is propagating along the guiding magnetic field.

Self-consistent boundary conditions at the magnetized beam surface require all field components. In the systems with magnetized beams, the normal modes are hybrid modes of TM and TE modes, even in the axisymmetric case. In order to designate the nonaxisymmetric hybrid modes, two letters of EH and HE are commonly used. However, the definition of EH and HE is rather arbitrary. In this paper, the definition in the field of the plasma physics is used, which is the same as Refs. [10-13]. By using the new version of self-consistent theory, the Cherenkov and slow cyclotron instability in the periodically corrugated cylindrical waveguide is studied for non-oversized BWO parameters [11, 12]. For oversized cases, the numerical calculation becomes very difficult as is discussed in Ref. [13], in which the field properties of the operation modes are numerically examined.

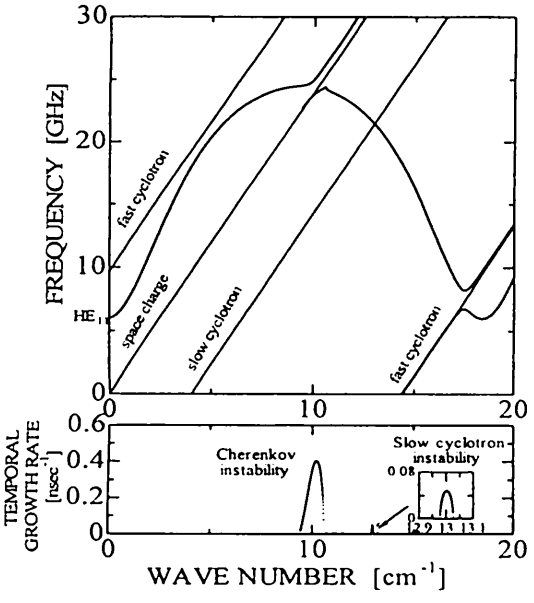

Fig.8 Dispersion characteristics of HE_{11} mode.

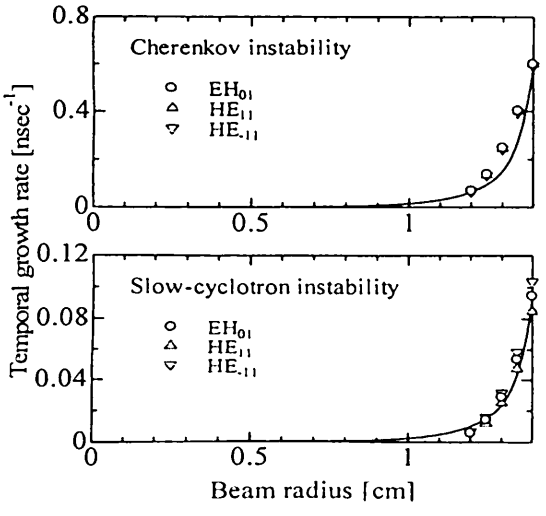

Fig.9 Dependence of the growth rate on the beam radius.

We improve the new version of numerical methods to analyze beam interactions in the oversized BWO. Figure 8 shows the dispersion characteristics of the nonaxisymmetric modes with m=1. The electromagnetic mode of SWS is the fundamental HE_{11} mode. Four beam modes exist on the axially streaming beam guided by a finite strength magnetic field. These are fast space charge mode, slow space charge mode, fast cyclotron mode and slow cyclotron mode. The slow space charge and slow cyclotron modes couple to HE_{11} mode, resulting in Cherenkov and slow cyclotron instabilities. The temporal growth rates of these instabilities are shown at the lower frame of Fig.8.

Figure 9 shows the dependence of the growth rate on the beam radius. The growth rates decrease exponentially as the beam is apart from the SWS wall. Since the perturbations is assumed to be $\exp[i(k_z z+m\theta-\omega t)]$, the electromagnetic field rotates rightward (leftward) in the laboratory frame of reference with positive (negative) m. For the oversized BWO, the growth rate of instability is not affected by the rotational direction. This is contrastive with the non-oversized BWO. For non-oversized cases, the rotational direction of electromagnetic wave strongly affects the instabilities [12]. The Cherenkov and slow cyclotron interactions become stronger compared with the non-oversized X-band BWO. The Cherenkov interaction may be responsible for the radiation of oversized BWO, because its growth rate is much larger than the slow cyclotron growth rate for our experimental parameters. Note that the nonaxisymmetric modes can be excited in the completely axisymmetric system as in Fig.7. In ref.[14], nonaxisymmetric mode and its coupling with axisymmetric modes are examined in a non-oversized traveling wave amplifier. The main interaction mode is TM_{01} and nonaxisymmetric mode is assumed to be excited by asymmetries of the system. According to our analysis, for the oversized BWOs cases, nonaxisymmetric modes may be excited and may become dominant operation mode, even in the completely symmetric system.

V. Summary

We study operation mode of oversized BWOs. The beam voltage is weakly relativistic, less than 100 kV. The beam current is in the range of 100-500 A. The output power increases if the beam interaction point approaches to the π point, by increasing the beam voltage. The performance of BWO also depends on the beam shape and radius. Since the electromagnetic fields in oversized BWOs are surface waves localized near the SWS wall, the beam needs to be uniformly distributed and to propagate near the SWS wall for the efficient operations.

The quality factor Pf^2 of both BWOs is about 2×10^4 [kW·GHz^2] in the range 40-50 kV. Its values increase by a factor of about 3 by increasing the beam voltage above 70 kV. The maximum output power is above 100 kW for the K-band BWO and about 50-60 kW for the Q-band BWO. At 90-100 kV with the improved beam and SWS, the radiatuion

power increases up to about 500 kW (K-band BWO) and 200 kW (Q-Band BWO). The quality factor Pf^2 is about 3.5×10^5 [kW·GHz^2]. The high-power operation of the oversized BWO is due to the Cherenkov instability. The beam interaction with the nonaxisymmetric mode is the same as the axisymmetric interaction. Hence, the nonaxisymmetric mode may become dominant mode, even in the completely symmetric system.

Acknowledgement

This work was partially supported by a Grant-in-Aid for Scientific Research from the Ministry of Education, Science, Sports and Culture of Japan. Support of numerical calculations was afforded by the Computer Center, National Institute for Fusion Science.

References

[1] J. Benford and J. Swegle: High-Power Microwaves, Artech House, Norwood, MA (1992).

[2] S. P. Bugaev, V. A. Cherepenin, V. I. Kanavets, V. I. Koshelev, V. A. Popov, and A. N. Vlasov: "Investigation of a Millimeter-Wavelength-Range Relativistic Diffraction Generator", IEEE Trans. Plasma Sci., vol.18, pp.518-524 (1990).

[3] S. P. Bugaev, V. A. Cherepenin, V. I. Kanavets, A. I. Klimov, A. D. Kopenkin, V. I. Koshelev, V. A. Popov, and A.I.Slepkov: "Relativistic Multiwave Cerenkov Generators", IEEE Trans. Plasma Sci., vol.18, pp.525-536 (1990).

[4] Md. R. Amin, K. Minami, K. Ogura, X. Z. Zheng, and T. Watanabe: "Resonant Enhancement of Radiation from a Backward Wave Oscillator Utilizing Large Diameter Corrugated Metal Structure", J. Phys. Soc. Jpn., vol.64, pp.4473-4484 (1995).

[5] K. Ogura, M. R. Amin, K. Minami, X. D. Zheng, Y. Suzuki, W. S. Kim, T. Watanabe, Y. Carmel, and V. L. Granatstein: "Experimental Demonstration of a High-Power Slow-Wave Electron Cyclotron Maser Based on a Combined Resonance of Cherenkov and Anomalous Doppler Interactions", Phys. Rev. E, vol.53, pp.2726-2729 (1996).

[6] A. N. Vlasov, A. G. Shkvarunets, J. C. Rodgers, Y. Carmel, T. M. Antonsen, Jr., T. M. Abuelfadl, D. Lingze, V. A. Cherepenin, G. S. Nusinovich, M. Botton, and V. L. Granatstein: "Overmoded GW-Class Surface-Wave Microwave Oscillator", IEEE Trans. Plasma Sci., vol.28, pp.550-560 (2000).

[7] K. Ogura, R. Yoshida, K. Komiyama, M. Sakai, and H. Yamazaki: "Experimental Demonstration of Mode Change in a Q-Band Oversized Backward Wave Oscillator due to Corrugation Number", IEEJ Trans. FM, vol.124, pp.456-460 (2004).

[8] K. Ogura, R. Yoshida, Y. Yamashita, H. Yamazaki, K. Komiyama, and M. Sakai: "Study on Oscillation Starting Condition of K-Band Oversized Backward Wave Oscillator Driven by a Weakly Relativistic Electron Beam", J. Plasma Fusion Res. SERIES, vol.6, pp.703-706 (2004).

[9] K. Ogura, K. Komiyama, M. Sakai, D. Yamada, H. Saito, and H. Yamazaki: "Performance of Weakly Relativistic Oversized Backward Wave Oscillators", IEEJ Trans. FM, vol.125, pp.733-738 (2005).

[10] O. Watanabe, K. Ogura, T. Cho, and Md. R. Amin: "Self-Consistent Linear Analysis of Slow Cyclotron and Cherenkov Instabilities", Phys. Rev. E, vol.63, pp.6503(1-9), 2001.

[11] H. Yamazaki, O. Watanabe, Y. Yamashita, M. Iwai, Y. Suzuki, and K. Ogura: "Cherenkov and Slow Cyclotron Instability in Periodically Corrugated Cylindrical Waveguide in Low Magnetic Field Region", IEEJ Trans., 124, pp.477-482 (2004).

[12] H. Yamazaki, M. Iwai, Y. Suzuki, H. Takagi, O. Watanabe, and K. Ogura: "Nonaxisymmetric Instabilities in Periodically Corrugated Cylindrical Waveguide with Low Magnetic Field", IEEJ Trans., 125, pp.739-743 (2005).

[13] H. Yamazaki, H. Takagi, H. Tanaka, and K. Ogura: "Numerical Examination of Operation Modes of Weakly Relativistic Oversized Backward Wave Oscillator", accepted for publication in J. Plasma Physics.

[14] S. Banna, J. A. Nation, L. Schachter, and P. Wang: "The Interaction of Symmetric and Asymmetric Modes in a High-Power Traveling-Wave Amplifier", IEEE Trans. Plasma Sci., vol.28, pp.798-811 (2000).

原稿受付日	平成 18 年 7 月 7 日